NeuroImage: Clinical 11 (2016) 133–138

Contents lists available at ScienceDirect

NeuroImage: Clinical

journal homepage: www.elsevier.com/locate/ynicl

Profiles of aberrant white matter microstructure in fragile X syndrome

Scott S. Hall[a,*], Robert F. Dougherty[b], Allan L. Reiss[a]

[a]Center for Interdisciplinary Brain Sciences Research, Department of Psychiatry and Behavioral Sciences, Stanford University School of Medicine, Stanford, CA, United States
[b]Center for Neurobiological Imaging (CNI), Stanford University, Stanford, CA, United States

ARTICLE INFO

Article history:
Received 24 July 2015
Received in revised form 9 January 2016
Accepted 12 January 2016
Available online 14 January 2016

Keywords:
Fragile X syndrome
White matter microstructure
Autism
FMR1 gene
Diffusion tensor imaging

ABSTRACT

Previous studies attempting to quantify white matter (WM) microstructure in individuals with fragile X syndrome (FXS) have produced inconsistent findings, most likely due to the various control groups employed, differing analysis methods, and failure to examine for potential motion artifact. In addition, analyses have heretofore lacked sufficient specificity to provide regional information. In this study, we used Automated Fiber-tract Quantification (AFQ) to identify specific regions of aberrant WM microstructure along WM tracts in patients with FXS that differed from controls who were matched on age, IQ and degree of autistic symptoms. Participants were 20 patients with FXS, aged 10 to 23 years, and 20 matched controls. Using Automated Fiber-tract Quantification (AFQ), we created Tract Profiles of fractional anisotropy and mean diffusivity along 18 major WM fascicles. We found that fractional anisotropy was significantly increased in the left and right inferior longitudinal fasciculus (ILF), right uncinate fasciculus, and left cingulum hippocampus in individuals with FXS compared to controls. Conversely, mean diffusivity was significantly decreased in the right ILF in patients with FXS compared to controls. Age was significantly negatively associated with MD values across both groups in 11 tracts. Taken together, these findings indicate that FXS results in abnormal WM microstructure in specific regions of the ILF and uncinate fasciculus, most likely caused by inefficient synaptic pruning as a result of decreased or absent Fragile X Mental Retardation Protein (FMRP). Longitudinal studies are needed to confirm these findings.

1. Introduction

FXS is the most common known inherited form of intellectual disability affecting approximately 1 in 3000 boys and 1 in 5000 girls worldwide (Hagerman, 2008). First described by Martin and Bell in 1943 as a "pedigree of mental defect showing sex linkage" (Martin and Bell, 1943), FXS is caused by mutations to the *FMR1* gene at locus 27.3 on the long arm of the X chromosome (Verkerk et al., 1991). Excessive methylation of the gene impairs production of Fragile X Mental Retardation Protein (FMRP), a key protein involved in synaptic plasticity and dendritic maturation in the brain (Greenough et al., 2001; Soden and Chen, 2010). As a result, individuals with FXS exhibit a specific profile of developmental and cognitive deficits (Reiss and Dant, 2003) including impairments in executive functioning, visual memory and perception, mental manipulation of visual–spatial relationships among objects, aberrant processing of arithmetical stimuli, as well as increased risk for autistic-like behaviors (e.g., social avoidance, communication impairments and repetitive behaviors) (Bennetto et al., 2001; Cornish et al., 2004; Dissanayake et al., 2009; Hall et al., 2006; Hall et al., 2009; Kaufmann et al., 2004; Mazzocco, 2001; Mazzocco et al., 2006; Murphy, 2009; Skinner et al., 2005; Sudhalter et al., 1990; Sullivan et al., 2007; Sullivan et al., 2006). However, data suggests that there are significant brain and behavioral differences between those diagnosed with FXS and those diagnosed with autism (Hall et al., 2009).

Over the past decade, studies employing diffusion tensor imaging (DTI) methods (Basser, 1995; Basser and Pierpaoli, 1996; Pierpaoli and Basser, 1996) have indicated that white-matter (WM) microstructure may be aberrant in individuals with FXS. For example, Barnea-Goraly and colleagues reported that fractional anisotropy (FA), which quantifies diffusion anisotropy, was significantly decreased in fronto-striatal pathways as well as in parietal sensory-motor tracts in 10 females with FXS, aged 13 to 22 years, compared to age-matched typically developing controls (Barnea-Goraly et al., 2003). In a more recent study, Villalon-Reina and colleagues (Villalon-Reina et al., 2013), reported that mean diffusivity (MD) — the average diffusion across all directions — was significantly increased in regions along the superior longitudinal fasciculus (SLF), inferior longitudinal fasciculus (ILF), and inferior fronto-occipital fasciculus (IFOF) in 18 girls with FXS, aged 7 to 14 years, compared to typically developing controls. Taken together, these studies suggest that FXS may be characterized by differences in tissue structure in long association WM tracts.

However, in studies in which patients with FXS are compared to neurotypical controls, it is unclear whether the differences in WM

* Corresponding author at: Center for Interdisciplinary Brain Sciences Research, Department of Psychiatry and Behavioral Sciences, Stanford University, 401 Quarry Road, Stanford, CA 94305-5795, United States.
E-mail address: hallss@stanford.edu (S.S. Hall).

http://dx.doi.org/10.1016/j.nicl.2016.01.013

microstructure are specific to FXS, or simply related to differences in IQ and other cognitive and behavioral symptoms between the groups. One way to overcome this problem is to compare individuals with FXS to those who have similar IQs and levels of autistic symptoms, but who do not have FXS. In a recent study from our group (Green et al., 2015), for example, the WM microstructure of patients with FXS (25 females, 15 males) was compared to non-FXS individuals who had similar levels of IQ and autistic symptoms. Using Tract-Based Spatial Statistics (TBSS) (Smith et al., 2006), mean FA values in the inferior longitudinal, inferior fronto-occipital and uncinate fasciculi were found to be significantly *increased* in patients with FXS compared to controls. However, these analyses lacked sufficient specificity to provide information concerning whether WM microstructure is abnormal along the whole tract or at specific locations on a tract.

Given the inconsistent findings, here we refine our analyses and study design in three ways. First, we employed a more granular method of fiber-tract quantification — Automated Fiber-tract Quantification (AFQ) (Yeatman et al., 2012a) — to identify regions of aberrant WM microstructure in these patients. Second, we compared patients with FXS to a well-matched group of individuals with idiopathic developmental disability (but who did not have FXS) in order to rule out age, IQ, and degree of autistic symptoms as possible confounds. Finally, we examined the degree to which subject movement may have influenced our findings.

2. Materials and methods

2.1. Participants

All participants had taken part in a previous study investigating large-scale brain networks in patients with FXS (Hall et al., 2013). There was no overlap of the participants studied here with a previous DTI study from our group (Green et al.). Patients with FXS were included if they were aged between 10 and 23 years, had an IQ between 50 and 90 points on the Wechsler Abbreviated Scale of Intelligence (WASI) (Wechsler, 1999), and could demonstrate that they could remain immobile for 10 min while lying in the scanner. During recruitment, control participants were matched to children with FXS in terms of age (+/−3 years), IQ (+/−10 points) and severity of autistic symptoms (+/−5 points on the Social Communication Questionnaire [SCQ]) (Rutter et al., 2003). Individuals in both groups were excluded from the study if they were born preterm (<34 weeks), had low birth weight (<2000 g), showed evidence of a genetic condition other than FXS, exhibited sensory impairments, or had any serious medical or neurological condition that affected growth or development (e.g., seizure disorder, diabetes, congenital heart disease). Finally, individuals were excluded if they had materials in their body that would preclude an MRI scan (e.g., dental braces). Control participants were subsequently screened for FXS to confirm that they did not have FXS. All protocols were approved by the human subjects committee at Stanford University School of Medicine and all parents gave consent for their child to participate in the study.

All participants with FXS had a confirmed genetic diagnosis of FXS (i.e., >200 CGG repeats on the *FMR1* gene and evidence of aberrant methylation) as evidenced by standard Southern Blot techniques. Two male participants with FXS were mosaic (i.e., an additional unmethylated fragment was detected in the premutation range). Five control participants had an additional co-morbid diagnosis (2 ADHD, 1 PTSD and 2 ASD). As can be seen from Table 1, the two groups were well matched in terms of age, IQ, and degree of autistic symptomatology (Table 1). Nine (45%) participants with FXS and 6 (30%) controls were taking psychoactive medications. In the FXS group, medications included sertraline (2 participants), venlafaxine (1 participant), donepezil (1 participant), aripiprazole (1 participant), and methylphenidate (3 participants). In the control group, medications included methylphenidate (5 participants), aripiprazole (2 participants), imipramine (1 participant), and arbaclofen (1 participant). As expected, mean IQs were significantly higher in females with FXS ($M = 73.0$, $SD = 8.0$) than in males with FXS ($M = 59.75$, $SD = 9.0$) [($t(18) = 3.21$, $p = .006$)]. There were, however, no other differences between female and male participants with FXS on the other measures. Within the FXS group, age and IQ were not associated with scores on the SCQ.

Table 1
Demographic information.

Characteristic	FXS *N* (%)	Controls *N* (%)	*P*
Total	20	20	
Female	12 (60.0)	7 (35.0)	*NS*
Medications (any)	9 (45.0)	6 (30.0)	*NS*
	Mean (SD)	Mean (SD)	
Age, year	16.63 (4.69)	16.57 (3.90)	*NS*
FSIQ[a]	67.30 (10.54)	64.85 (11.03)	*NS*
Autistic symptoms[b]	8.90 (5.72)	11.15 (6.63)	*NS*

Abbreviations: FXS, fragile X syndrome; FSIQ, full scale IQ; VIQ, verbal IQ; PIQ, Performance IQ.
[a] Wechsler Abbreviated Scale of Intelligence (Wechsler, 1999).
[b] Social Communication Questionnaire (Rutter et al., 2003).

2.2. Diffusion weighted imaging acquisition and processing

Diffusion weighted imaging (DWI) data were acquired immediately following a blood oxygen level dependent (BOLD) resting-state MRI scan on a 3.0-T whole-body MRI scanner (GE Medical Systems, Milwaukee, WI) with the vendor-supplied 8-channel receive coil at Stanford University. A diffusion-weighted, single-shot, spin-echo, echoplanar imaging sequence (TE = 72.7 ms, TR = 5.7 s, FOV = 240 mm, matrix size = 128 × 128) was used to acquire 44 2.9 mm-thick slices in 23 different diffusion directions (b = 850) for a voxel size of 1.9 × 1.9 × 2.9 mm. The sequence was repeated four times and six non-diffusion weighted (b = 0) volumes were collected (total scan duration was 8 min). Eddy current distortions and subject motion in the diffusion weighted images were removed by a 14-parameter constrained non-linear co-registration based on the expected pattern of eddy-current distortions given the phase-encode direction of the acquired data (Rohde et al., 2004). Each diffusion-weighted image was registered to the mean of the (motion-corrected) non-diffusion-weighted (b = 0) images using a two-stage coarse-to-fine approach that maximized the normalized mutual information. The mean of the non-diffusion-weighted images was automatically aligned to the T1 image using a rigid body mutual information algorithm. All raw images from the diffusion sequence were resampled to 2-mm isotropic voxels by combining the motion correction, eddy-current correction, and anatomical alignment transforms into one omnibus transform and resampling the data using a trilinear interpolation algorithm based on code from SPM5 (Friston and Ashburner, 2004). An eddy-current intensity correction was applied to the diffusion-weighted images at the resampling stage (Rohde et al., 2004).

The rotation component of the omnibus coordinate transform was applied to the diffusion-weighting gradient directions to preserve their orientation with respect to the resampled diffusion images. The tensors were then fit using a robust least-squares algorithm designed to remove outliers from the tensor estimation step (Chang et al., 2005). We computed the eigenvalue decomposition of the diffusion tensor and the resulting eigenvalues were used to compute fractional anisotropy (FA) and mean diffusivity (MD) (Basser and Pierpaoli, 1996). All the custom image processing software are from the open-source mrDiffusion package, available for download from http://github.com/vistalab/vistasoft/.

Table 2
Group differences in tract diffusion properties.

Tract name	Fractional anisotropy (FA)		Mean diffusivity (MD)	
	F	*p*	*F*	*p*
Left ILF	**4.38**	**.044**	2.13	.153
Right ILF	**6.61**	**.015**	**10.12**	**.003**
Left SLF	3.64	.065	.49	.488
Right SLF	.74	.395	.12	.731
Left IFOF	.11	.738	.14	.707
Right IFOF	.24	.628	.11	.744
Left cingulum hippocampus	**4.24**	**.049**	.26	.617
Right cingulum hippocampus	.44	.510	.70	.410
Left thalamic radiation	.01	.924	.74	.394
Right thalamic radiation	.09	.767	.43	.516
Left cingulum cingulate	.24	.628	.00	.981
Right cingulum cingulate	.54	.469	.04	.839
Callosum forceps major	.01	.916	1.87	.180
Callosum forceps minor	1.64	.208	1.22	.277
Left uncinate	1.08	.305	.59	.449
Right uncinate	**10.09**	**.003**	.05	.818
Left arcuate	.09	.765	.18	.671
Right arcuate	.05	.833	.20	.655

Bold indicates $p < .05$.

2.3. Fiber tract identification

We used the AFQ software package for the automatic identification and quantification of cerebral WM pathways (Yeatman et al., 2012a). AFQ uses a three-step procedure to identify 18 major fiber tracts in an individual's brain: (1) fiber tractography, (2) waypoint region-of-interest (ROI)-based fiber tract segmentation and (3) fiber tract refinement based on a probabilistic fiber tract atlas. Each fiber group was summarized with a vector of 100 nodes representing the diffusion properties sampled at equidistant locations along the tract — i.e., a "Tract Profile". Only the portion of the tract between the two defining ROIs was analyzed. This was done in order to achieve better alignment of the Tract Profiles across subjects.

2.4. Individual and group level inference

We conducted separate three-way mixed-design analyses of covariance (ANCOVA) for the continuous dependent variables (FA and MD) with node as a repeated measures factor and group and sex as between-group factors. Participant age was included as a continuous covariate. Follow-up Bonferroni-corrected comparisons were used to further investigate significant main-effects and interactions identified in the omnibus tests. For all Tract Profile analyses, results are expressed as mean ± SEM (standard error of the mean), and a p-value less than 0.05 (Bonferroni-corrected), was considered statistically significant. To examine potential head motion artifacts, we calculated the average volume-by-volume translation (in mm) and the average volume-by-volume rotation (in degrees) across each scan for each participant (Yendiki et al., 2013) and computed correlations with the diffusion parameters for each tract where we had obtained significant differences between the groups.

3. Results

3.1. Effects of group

F statistics evaluating mean differences between the groups in FA and MD for each of the 18 major WM tracts identified by AFQ are shown in Table 2. The table shows that, compared to controls, patients with FXS obtained significantly higher mean FA values in the left ILF ($F = 4.38$, $p = .044$), right ILF ($F = 6.61$, $p = .015$), left cingulum hippocampus ($F = 4.24$, $p = .049$) and right uncinate fasciculus ($F = 10.09$, $p = .003$). Patients with FXS also obtained significantly lower mean MD values in the right ILF ($F = 10.12$, $p = .003$) compared to controls.

Figs. 1 and 2 show Tract Profiles generated for the tracts where significant differences in means were obtained between the groups in FA (Fig. 1) and MD (Fig. 2). As can be seen from the plots, FA and MD values

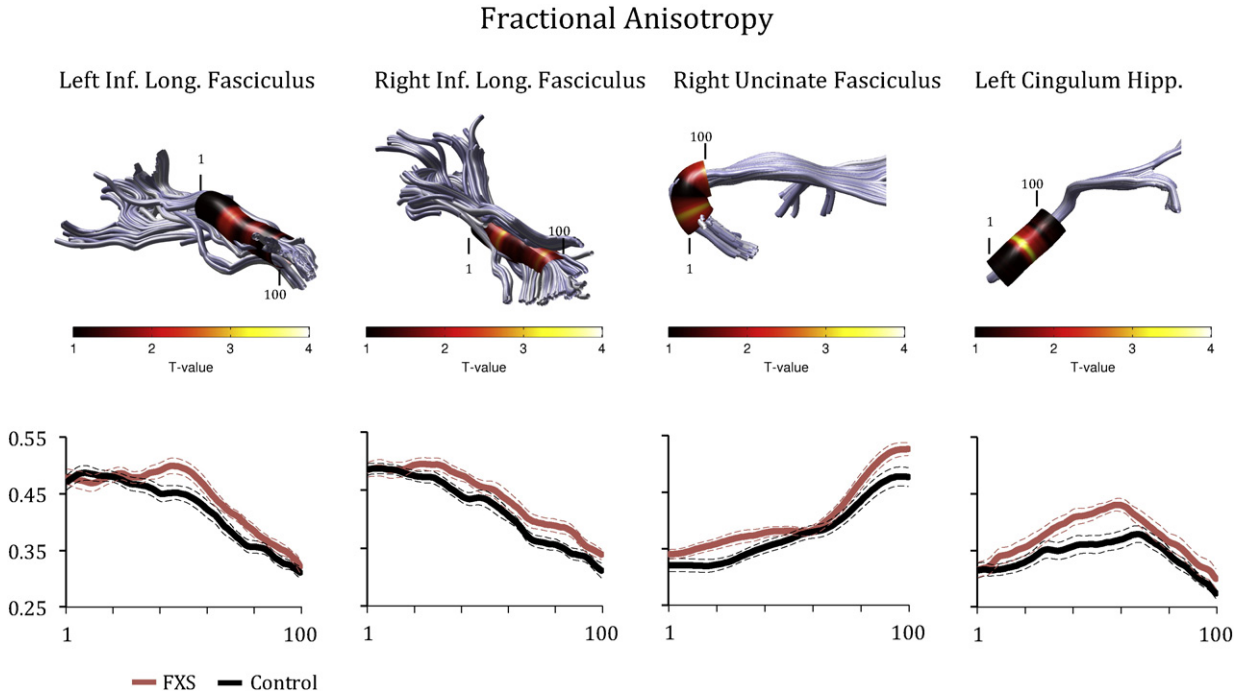

Fig. 1. Group differences in fractional anisotropy (FA) in the Left ILF, right ILF, uncinate fasciculus and cingulate hippocampus. The color bar indicates T-statistic values from Bonferroni-corrected analyses of covariance conducted at each location along the tract length. Each Tract Profile shows FA values calculated at each of 100 equidistant points (x-axis) along the fascicle for individuals with FXS (represented in red), and matched controls (represented in black). Each plot shows the mean Tract Profile +/− 1 standard error of the mean for each group.

varied substantially along each tract, indicating that mean differences in FA and MD could have obscured localized effects. ANCOVA analyses indicated that higher FA values in patients with FXS were obtained primarily in the middle section of the ILF, the anterior and posterior sections of the right uncinate, and the middle section of the left cingulum hippocampus (Fig. 1). Lower MD values were obtained primarily in the middle section of the right ILF in patients with FXS (Fig. 2).

3.2. Effects of sex

There were no differences between male and female participants in terms of FA values obtained on each tract. However, female participants were found to exhibit significantly elevated MD values in the right uncinate compared to male participants ($F = 4.796$, $p = .035$). There was also a significant interaction between sex and group in the right uncinate for the FA values ($F = 4.18$, $p = .049$). Corrected comparisons revealed that control group females had significantly lowered FA values compared to males in either group ($p < .05$).

3.3. Effect of age

There was a significant main effect of age on FA values in the cingulum cingulate ($F = 5.70$, $p = .023$). Further examination of the data revealed that FA values in the cingulum were significantly positively correlated with age, indicating that FA values increased with age in this specific tract only. Conversely, there were significant main effects of age on MD values in 11 tracts: the left and right uncinate, left ILF, left and right SLF, left and right IFOF, right cingulum hippocampus, right thalamic radiation and left and right arcuate fasciculus. Further examination revealed that all MD values were significantly negatively correlated with age, indicating that MD values decreased significantly with age in these tracts.

3.4. Effects of subject motion

There were no differences between the groups in terms of the average volume-by-volume translation [FXS group: 2.66 mm (SD = .90 mm); control group: 2.50 mm ($SD = 1.13$ mm), $t(38) = .49$, $p = .63$] or average volume-by-volume rotation [FXS group: 1.07 degrees (SD = .39 degrees); control group: 1.15 degrees (SD = .66 degrees), $t(38) = .48$, $p = .63$]. In participants with FXS only, age was negatively correlated with average volume-by-volume translation ($r(20) = -.553$, $p = .011$) and average volume-by-volume rotation ($r(20) = -.47$, $p = .037$). Similarly, in participants with FXS only, total SCQ score was positively correlated with average volume-by-volume translation ($r(20) = .466$, $p = .038$) and average volume-by-volume rotation ($r(20) = .512$, $p = .021$). These data indicated that younger participants with FXS and those who had higher levels of autistic symptoms were more likely to exhibit head movements. There were no differences between males and females with FXS in subject motion. Fig. 3 shows the correlations obtained between the motion parameters and the diffusion parameters for each tract where we had obtained significant differences between the groups. The correlations between translational motion and FA values in the left cingulum hippocampus were the most positive (approaching 0.6) toward the middle of the tract. It is therefore possible that group differences obtained along this tract were influenced by subject motion.

4. Discussion

We identified regions of aberrant WM microstructure in patients with FXS that differed from individuals who did not have FXS but who were similar in age, IQ, and autistic symptomatology using a sophisticated method of fiber-tract identification (Automated Fiber-tract Quantification). To our knowledge, this is the first time that AFQ has been employed to identify aberrant WM microstructure in a neurogenetic disorder associated with autism. AFQ has a number of advantages over other methods including a complete and automated data processing pipeline that runs from raw DTI data to fiber tract identification, as well as the generation of "Tract Profiles" for 18 major fiber tracts, allowing us to identify specific locations along a tract that may be

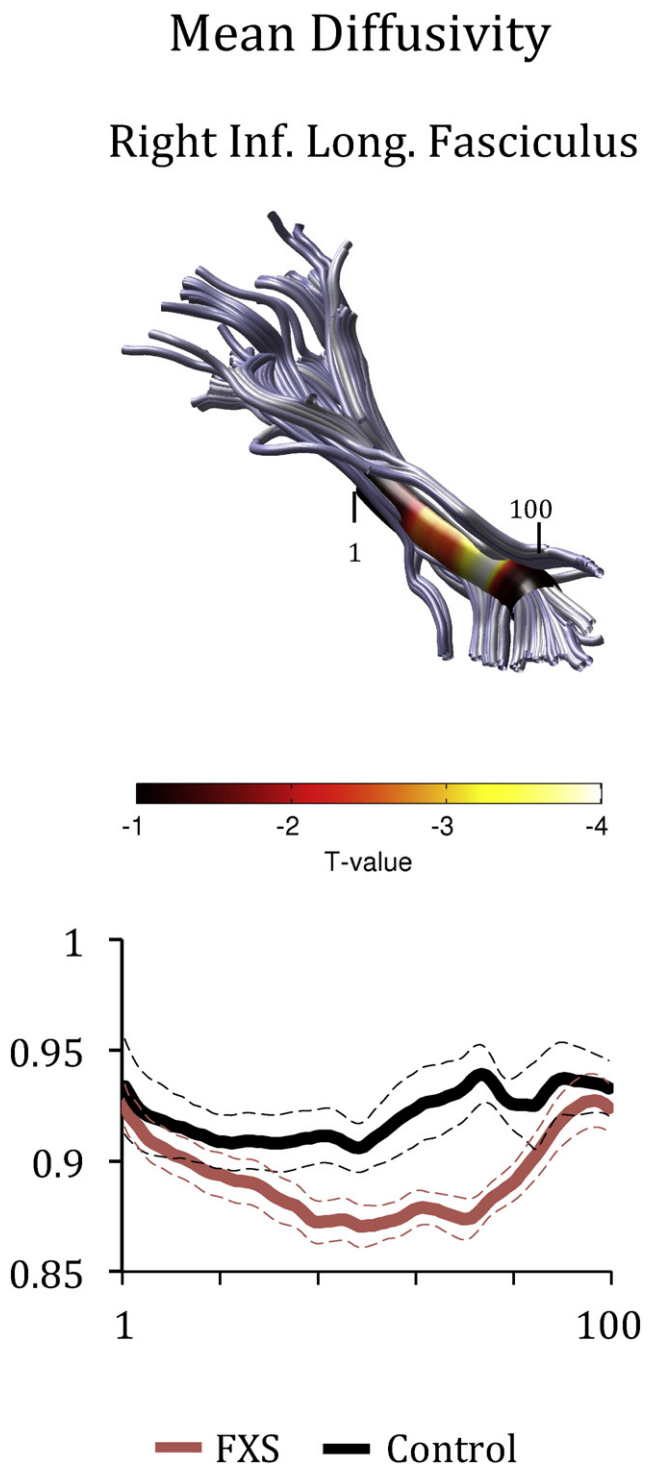

Fig. 2. Group differences in mean diffusivity (MD) in the right ILF. The color bar indicates T-statistic values from Bonferroni-corrected analyses of covariance conducted at each location along the tract length. The Tract Profile shows MD values calculated at each of 100 equidistant points (x-axis) along the fascicle for individuals with FXS (represented in red), and matched controls (represented in black). Each plot shows the mean Tract Profile +/− 1 standard error of the mean for each group.

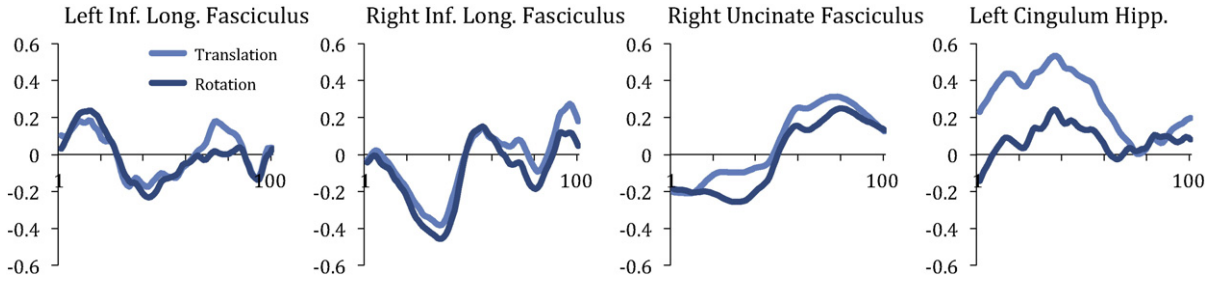

Fig. 3. Correlations obtained between diffusion parameters and subject motion (translation and rotation) along the length of the tracts where group differences were found.

abnormal in FXS. Previous studies have employed AFQ to examine WM microstructure in neurotypical individuals (Feldman et al., 2012), individuals with reading impairments (Yeatman et al., 2012b) and those born prematurely (Johnson et al., 2013), and these studies have shown that AFQ is an extremely robust and valid analysis technique.

Overall, the results showed that FA was significantly increased in patients with FXS in the left and right ILF, right uncinate fasciculus and left cingulum hippocampus compared to controls. Furthermore, MD was significantly decreased in the right ILF in patients with FXS compared to controls. Examination of the Tract Profiles revealed that FA and MD values varied quite substantially along each tract. Thus, in previous studies employing other DTI analysis methods, it is possible that statistical averaging of the FA and MD values across the length of each tract may have obscured potential region-specific differences along a tract. When the groups were compared at specific locations along each tract, we found that group differences (increased FA and decreased MD values) occurred primarily at the middle section of the left ILF and toward the frontal and posterior sections of the right uncinate, as well as toward the middle section of the left cingulum hippocampus. These data indicated that the Tract Profile analyses revealed important region-specific differences along specific sections of these tracts.

It is interesting to speculate upon why patients with FXS evidenced significantly increased FA (and decreased MD) in these specific tracts as opposed to decreased FA (and increased MD) values. In two previous studies, FA values were found to be decreased (Barnea-Goraly et al., 2003) and MD values were increased (Villalon-Reina et al., 2013) when girls with FXS were compared to neurotypical individuals. Given that WM maturation may depend on at least two opposing processes —myelination and pruning (Yeatman et al., 2012b) and that FMRP is thought to regulate synaptogenesis (Berry-Kravis et al., 2011), our findings suggest that aberrant synaptogenesis could result in reduced branching in these specific WM tracts in FXS leading to the increased FA values and decreased MD values.

Interestingly, our findings support a recent study from our group in which DTI was conducted on a non-overlapping cohort of patients with FXS of similar age (Green et al., 2015). In that study, a confirmatory analysis of specific WM tracts using TRACULA (Yendiki et al., 2011) indicated that mean FA values were significantly increased in the left ILF in patients with FXS compared to IQ-matched controls. Given that male toddlers with FXS have also been shown to have increased white matter fiber density compared to IQ-matched controls (Haas et al., 2009), it seems likely that aberrant pruning due to lack of FMRP in FXS may lead to axon growth dysregulation, thus producing the increased FA values. It is also possible that subject motion effects could have influenced the results. For example, we found that younger patients were FXS were more likely to exhibit increased head motion, as were patients with FXS who had higher levels of autistic symptoms. Although both groups were comparable in terms of the average volume-by-volume rotation and average volume-by-volume translation measured across scans, examination of the extent to which subject motion was correlated with diffusion parameters along the nodes of each tract revealed that translational motion was significantly correlated with FA values along the cingulum hippocampus. It is possible therefore that subject motion could have accounted for the differences observed between the groups in this tract. Interestingly, across both groups, we found that MD values decreased with increasing age in the majority of WM tracts. To determine whether the decrease in MD values may be related to intellectual disability in general, we would need to have included a group of typically developing children.

5. Conclusions

We have shown that FXS results in aberrant WM microstructure at specific locations along the ILF, uncinate fasciculus and cingulate hippocampus. The specificity of the present findings, combined with confirmatory findings by Green and colleagues, suggests that FXS is characterized by deficits in specific sections of WM tracts as a result of reduced FMRP. Although a number of Phase II clinical trials are now underway to evaluate pharmacological agents targeted to the downstream effects of reduced FMRP in FXS (Berry-Kravis et al., 2011), investigators have struggled to identify appropriate, reliable and sensitive outcome measures to track treatment efficacy. Given the specificity of the current findings, it may be possible to employ DTI as an imaging outcome measure in future clinical trials.

Acknowledgments

We thank Melissa Hirt, Ryan Kelley, Kristin Hustyi and Dr. Jennifer Hammond at Stanford University for their assistance with recruitment and scanning. This study was funded by grant K08MH081998 (Dr Hall) from the National Institutes of Health. The funder had no role in the design and conduct of the study; collection, management, analysis, and interpretation of the data; and preparation, review, or approval of the manuscript; and decision to submit the manuscript for publication.

The authors report no conflicts of interest.

References

Barnea-Goraly, N., Eliez, S., Hedeus, M., Menon, V., White, C.D., Moseley, M., Reiss, A.L., 2003. White matter tract alterations in fragile X syndrome: preliminary evidence from diffusion tensor imaging. Am. J. Med. Genet. B Neuropsychiatr. Genet. 118B (1), 81–88. http://dx.doi.org/10.1002/ajmg.b.10035.

Basser, P.J., 1995. Inferring microstructural features and the physiological state of tissues from diffusion-weighted images. NMR Biomed. 8 (7–8), 333–344.

Basser, P.J., Pierpaoli, C., 1996. Microstructural and physiological features of tissues elucidated by quantitative-diffusion-tensor MRI. J. Magn. Reson. B 111 (3), 209–219.

Bennetto, L., Taylor, A.K., Pennington, B.F., Porter, D., Hagerman, R.J., 2001. Profile of cognitive functioning in women with the fragile X mutation. Neuropsychology 15 (2), 290–299.

Berry-Kravis, E., Knox, A., Hervey, C., 2011. Targeted treatments for fragile X syndrome. J. Neurodev. Disord. 3 (3), 193–210.

Chang, L.C., Jones, D.K., Pierpaoli, C., 2005. RESTORE: robust estimation of tensors by outlier rejection. Magn. Reson. Med. 53 (5), 1088–1095. http://dx.doi.org/10.1002/mrm.20426.

Cornish, K.M., Turk, J., Wilding, J., Sudhalter, V., Munir, F., Kooy, F., Hagerman, R., 2004. Annotation: deconstructing the attention deficit in fragile X syndrome: a developmental neuropsychological approach. J. Child Psychol. Psychiatry 45 (6), 1042–1053.

Dissanayake, C., Bui, Q., Bulhak-Paterson, D., Huggins, R., Loesch, D.Z., 2009. Behavioural and cognitive phenotypes in idiopathic autism versus autism associated with fragile X syndrome. J. Child Psychol. Psychiatry 50 (3), 290–299.

Feldman, H.M., Lee, E.S., Yeatman, J.D., Yeom, K.W., 2012. Language and reading skills in school-aged children and adolescents born preterm are associated with white matter properties on diffusion tensor imaging. Neuropsychologia 50 (14), 3348–3362. http://dx.doi.org/10.1016/j.neuropsychologia.2012.10.014.

Friston, K.J., Ashburner, J., 2004. Generative and recognition models for neuroanatomy. NeuroImage 23 (1), 21–24. http://dx.doi.org/10.1016/j.neuroimage.2004.04.021.

Green, T., Barnea-Goraly, N., Raman, M., Hall, S.S., Lightbody, A.A., Bruno, J.L., et al., 2015. Specific effect of fragile-X mental retardation-1 on white matter microstructure. Br. J. Psychiatry.

Greenough, W.T., Klintsova, A.Y., Irwin, S.A., Galvez, R., Bates, K.E., Weiler, I.J., 2001. Synaptic regulation of protein synthesis and the fragile X protein. Proc. Natl. Acad. Sci. U. S. A. 98 (13), 7101–7106.

Haas, B.W., Barnea-Goraly, N., Lightbody, A.A., Patnaik, S.S., Hoeft, F., Hazlett, H., et al., 2009. Early white-matter abnormalities of the ventral frontostriatal pathway in fragile X syndrome. Dev. Med. Child Neurol. 51 (8), 593–599. http://dx.doi.org/10.1111/j.1469-8749.2009.03295.x.

Hagerman, P.J., 2008. The fragile X prevalence paradox. J. Med. Genet. 45 (8), 498–499.

Hall, S.S., Debernardis, G.M., Reiss, A.L., 2006. Social escape behaviors in children with fragile X syndrome. J. Autism Dev. Disord. 36, 935–947.

Hall, S.S., Lightbody, A.A., Huffman, L.C., Lazzeroni, L.C., Reiss, A.L., 2009. Physiological correlates of social avoidance behavior in children and adolescents with fragile x syndrome. J. Am. Acad. Child Adolesc. Psychiatry 48 (3), 320–329.

Hall, S.S., Jiang, H., Reiss, A.L., Greicius, M.D., 2013. Identifying large-scale brain networks in fragile x syndrome. JAMA Psychiatry 70 (11), 1215–1223. http://dx.doi.org/10.1001/jamapsychiatry.2013.247.

Johnson, R.T., Yeatman, J.D., Wandell, B.A., Buonocore, M.H., Amaral, D.G., Nordahl, C.W., 2013. Diffusion properties of major white matter tracts in young, typically developing children. NeuroImage 88C, 143–154. http://dx.doi.org/10.1016/j.neuroimage.2013.11.025.

Kaufmann, W.E., Cortell, R., Kau, A.S., Bukelis, I., Tierney, E., Gray, R.M., et al., 2004. Autism spectrum disorder in fragile X syndrome: communication, social interaction, and specific behaviors. Am. J. Med. Genet. A 129A (3), 225–234.

Martin, J.P., Bell, J., 1943. A pedigree of mental defect showing sex-linkage. Journal of Neurology and Psychiatry 6 (3–4), 154–157.

Mazzocco, M.M., 2001. Math learning disability and math LD subtypes: evidence from studies of Turner syndrome, fragile X syndrome, and neurofibromatosis type 1. J. Learn. Disabil. 34 (6), 520–533.

Mazzocco, M.M., Singh Bhatia, N., Lesniak-Karpiak, K., 2006. Visuospatial skills and their association with math performance in girls with fragile X or Turner syndrome. Child Neuropsychol. 12 (2), 87–110.

Murphy, M.M., 2009. A review of mathematical learning disabilities in children with fragile X syndrome. Dev. Disabil. Res. Rev. 15 (1), 21–27.

Pierpaoli, C., Basser, P.J., 1996. Toward a quantitative assessment of diffusion anisotropy. Magn. Reson. Med. 36 (6), 893–906.

Reiss, A.L., Dant, C.C., 2003. The behavioral neurogenetics of fragile X syndrome: analyzing gene–brain–behavior relationships in child developmental psychopathologies. Dev. Psychopathol. 15 (4), 927–968.

Rohde, G.K., Barnett, A.S., Basser, P.J., Marenco, S., Pierpaoli, C., 2004. Comprehensive approach for correction of motion and distortion in diffusion-weighted MRI. Magn. Reson. Med. 51 (1), 103–114. http://dx.doi.org/10.1002/mrm.10677.

Rutter, M., Bailey, A., Lord, C., 2003. The Social Communication Questionaire. Manual. Western Psychological Services, Los Angeles.

Skinner, M., Hooper, S., Hatton, D.D., Roberts, J., Mirrett, P., Schaaf, J., et al., 2005. Mapping nonverbal IQ in young boys with fragile X syndrome. Am. J. Med. Genet. A 132A (1), 25–32.

Smith, S.M., Jenkinson, M., Johansen-Berg, H., Rueckert, D., Nichols, T.E., Mackay, C.E., et al., 2006. Tract-based spatial statistics: voxelwise analysis of multi-subject diffusion data. NeuroImage 31 (4), 1487–1505. http://dx.doi.org/10.1016/j.neuroimage.2006.02.024.

Soden, M.E., Chen, L., 2010. Fragile X protein FMRP is required for homeostatic plasticity and regulation of synaptic strength by retinoic acid. J Neurosci 30 (50), 16910–16921. http://dx.doi.org/10.1523/JNEUROSCI.3660-10.2010.

Sudhalter, V., Cohen, I.L., Silverman, W., Wolf-Schein, E.G., 1990. Conversational analyses of males with fragile X, down syndrome, and autism: comparison of the emergence of deviant language. Am. J. Ment. Retard. 94 (4), 431–441.

Sullivan, K., Hatton, D., Hammer, J., Sideris, J., Hooper, S., Ornstein, P., Bailey Jr., D., 2006. ADHD symptoms in children with FXS. Am. J. Med. Genet. A 140 (21), 2275–2288.

Sullivan, K., Hatton, D.D., Hammer, J., Sideris, J., Hooper, S., Ornstein, P.A., Bailey Jr., D.B., 2007. Sustained attention and response inhibition in boys with fragile X syndrome: measures of continuous performance. Am. J. Med. Genet. B Neuropsychiatr. Genet. 144B (4), 517–532.

Verkerk, A.J., Pieretti, M., Sutcliffe, J.S., Fu, Y.H., Kuhl, D.P., Pizzuti, A., et al., 1991. Identification of a gene (FMR-1) containing a CGG repeat coincident with a breakpoint cluster region exhibiting length variation in fragile X syndrome. Cell 65 (5), 905–914.

Villalon-Reina, J., Jahanshad, N., Beaton, E., Toga, A.W., Thompson, P.M., Simon, T.J., 2013. White matter microstructural abnormalities in girls with chromosome 22q11.2 deletion syndrome, fragile X or Turner syndrome as evidenced by diffusion tensor imaging. NeuroImage 81, 441–454. http://dx.doi.org/10.1016/j.neuroimage.2013.04.028.

Wechsler, D., 1999. The Wechsler Abbreviated Scale of Intelligence Scale. The Psychological Corporation, San Antonio, TX.

Yeatman, J.D., Dougherty, R.F., Myall, N.J., Wandell, B.A., Feldman, H.M., 2012a. Tract profiles of white matter properties: automating fiber-tract quantification. PLoS One 7 (11), e49790. http://dx.doi.org/10.1371/journal.pone.0049790.

Yeatman, J.D., Dougherty, R.F., Ben-Shachar, M., Wandell, B.A., 2012b. Development of white matter and reading skills. Proc. Natl. Acad. Sci. U. S. A. 109 (44), E3045–E3053. http://dx.doi.org/10.1073/pnas.1206792109.

Yendiki, A., Panneck, P., Srinivasan, P., Stevens, A., Zollei, L., Augustinack, J., et al., 2011. Automated probabilistic reconstruction of white-matter pathways in health and disease using an atlas of the underlying anatomy. Front. Neuroinform. 5, 23. http://dx.doi.org/10.3389/fninf.2011.00023.

Yendiki, A., Koldewyn, K., Kakunoori, S., Kanwisher, N., Fischl, B., 2013. Spurious group differences due to head motion in a diffusion MRI study. NeuroImage 88C, 79–90. http://dx.doi.org/10.1016/j.neuroimage.2013.11.027.